DOI: 10.21062/mft.2023.092 http://www.journalmt.com

Hydrogen Embrittlement of 11SMn30 Free-Cutting Steel

Lukáš Šikyňa (0009-0004-7168-6852), František Nový (0000-0002-7527-5020), Peter Palček (0000-0001-7902-2007), Petra Drímalová (0000-0001-8461-9529), Martin Slezák (0009-0008-3181-0862), Milan Uhríčik (0000-0002-2782-5876), Veronika Chvalníková (0009-0002-1523-8065)
Faculty of Mechanical Engineering, Department of Materials Engineering, University of Žilina, Univerzitná 8215/1, 010 26 Žilina, Slovakia, E-mail: lukas.sikyna@fstroj.uniza.sk, frantisek.novy@fstroj.uniza.sk, peter.palcek@fstroj.uniza.sk, petra.drimalova@fstroj.uniza.sk, martin.slezak@fstroj.uniza.sk, milan.uhricik@fstroj.uniza.sk, veronika.chvalnikova@fstroj.uniza.sk

The main objective of the work was to describe the laboratory methods suitable for the hydrogenation of free-cutting steels. Furthermore, to study the hydrogen embrittlement of 11SMn30 free-cutting steel. Hydrogenation and subsequent mechanical testing of hydrogenated steel is not a common laboratory method as it requires precise and expensive equipment and is time-consuming and dangerous as hydrogen is highly reactive and explosive. Currently, several theories of hydrogen embrittlement mechanisms of steels describe the causes of material degradation by hydrogen. However, those theories are not universally valid; individual accounts have been developed and describe hydrogen embrittlement only for specific conditions and may fail in their descriptions under others. In this work, the hydrogenation of free-cutting steel 11SMn30 steel by two different methods (immersion and cathodic) was investigated to induce embrittlement and to compare in particular the fracture surfaces after the Charpy impact test. The results reported in this paper indicate that manganese sulphide inclusions are not the main cause of hydrogen embrittlement in free-cutting steels. The effect of manganese sulphide inclusions was attributed only to hydrogen trapping, that generated a high stress causing their decohesion from the matrix.

Keywords: Hydrogen embrittlement, Free-cutting steel, Fracture, Mechanical testing

1 Introduction

The increased presence of hydrogen in structural materials leads to many changes in the material properties of all structural metallic materials. In most cases, mechanical properties decrease. The presence of hydrogen in the material structure also results in a deterioration of the material's resistance to brittle failure due to the change in the failure mechanism. Atomic hydrogen can induce hydrogen embrittlement in the material. Hydrogen embrittlement of the material is manifested at both normal and low temperatures. On the other hand, dissolved hydrogen can react with carbon or other elements at higher temperatures to induce hydrogen embrittlement in the material [1, 2]. Due to its very small size, atomic hydrogen can diffuse intensively into the surface layers of the material. Even in very small quantities, hydrogen can cause damage to the material. The negative effect is already visible at a concentration of 0.0001 weight % of hydrogen in the material, at which point it is capable of initiating cracks [2, 3]. If molecular hydrogen is generated and accumulates in structural defects such as pores, inclusions or grain boundaries, the material becomes brittle and starts to crack. The hydrogen atoms in the material combine to form the H_2 molecule, creating pressures on the order of 10,000 MPa [2, 4].

So-called free-cutting steels belong among the group of plain carbon steels. Depending on the requirements that the steel has to meet, they can be supplied as soft free-cutting steels, which are not suitable for the production of hardened, case-hardened and surface-hardened components, and quenched and tempered free-cutting steels which are recommended for high-load parts. Soft free-cutting steels are supplied in bars or rolls without heat treatment. Because of superior machinability, they are intended for the mass production of low-load small parts (connecting and fastening elements, threaded hydraulic components, fittings) using automatic machines with high metal removal rates. They have been specially designed to be machined by chip removal with high productivity because form small chips when machined. In contrast, mild steels form tough chips that form long spirals and thus make the machining more difficult. Machining of free-cutting steels is characterized by good machinability and easy chip fragmentation (good surface quality at high cutting speed). This grade of steel is characterised by

a carbon ratio ranging from 0.007% to 0.60%, sulphur ratio from 0.15% to 0.40 % and phosphorus ratio from 0.07% to 0.10%. Higher content of sulphur and phosphorus, impair the toughness of the steel and thus promote chip fragmentation during the machining. It is important to eliminate the harmful effect of sulphur by increasing the manganese content (up to 1.1 %) [5, 6]. Production of free-cutting steels must be monitored to achieve uniform distribution of sulphide inclusion throughout the cross-section [7]. On the other hand, the presence of manganese sulphide inclusions is crucial for good machinability, but causes increased susceptibility of steel to hydrogen embrittlement, because specific distributions of non-metallic inclusions or grain boundary particles in steels result in increased susceptibility to hydrogen embrittlement.

The purpose of this paper was to experimentally explore the susceptibility of 11SMn30 steel to hydrogen embrittlement, because this soft free-cutting steel is also used for the production of various components that come into contact with media containing atomic hydrogen.

2 Experimental material

The investigated material (11SMn30 steel) was delivered in the form of small specimens of dimensions 10x10x55 mm in quantity of 10 pcs. The material was supplied by HYDAC Electronics which, among other things, uses free-cutting steels for the production of various components that come into contact with hydrogen media. In the middle of these "prisms" the "V" notches were made for impact bending test. The Charpy impact test was key to obtaining the fracture surfaces which were the main object of interest in determining how much the material degraded due to the hydrogen embrittlement. To define the initial state of the material under investigation, its chemical composition was determined first.

The chemical analysis of the tested material was carried out using a SPECTROMAXx light emission spectrometer with a wavelength range of 140-670nm. To verify the accuracy of the results a handheld SpectroSort X-ray spectrometer was used also [8]. The measured chemical composition of 11SMn30 steel is given in Tab.1 and was compared with the standard composition (Tab. 2).

Tab. 1 *Chemical composition in wt. % of the experimental material*

C	Si	Mn	P	S
0.120	0.0167	1.32	0.0671	0.120

Tab. 2 *Chemical composition in wt. % of steel 11SMn30 (1.0715): EN 10277-3-2008*

C	Si	Mn	P	S
max. 0.14	max. 0.05	0.9 - 1.3	max. 0.11	0.27 - 0.33

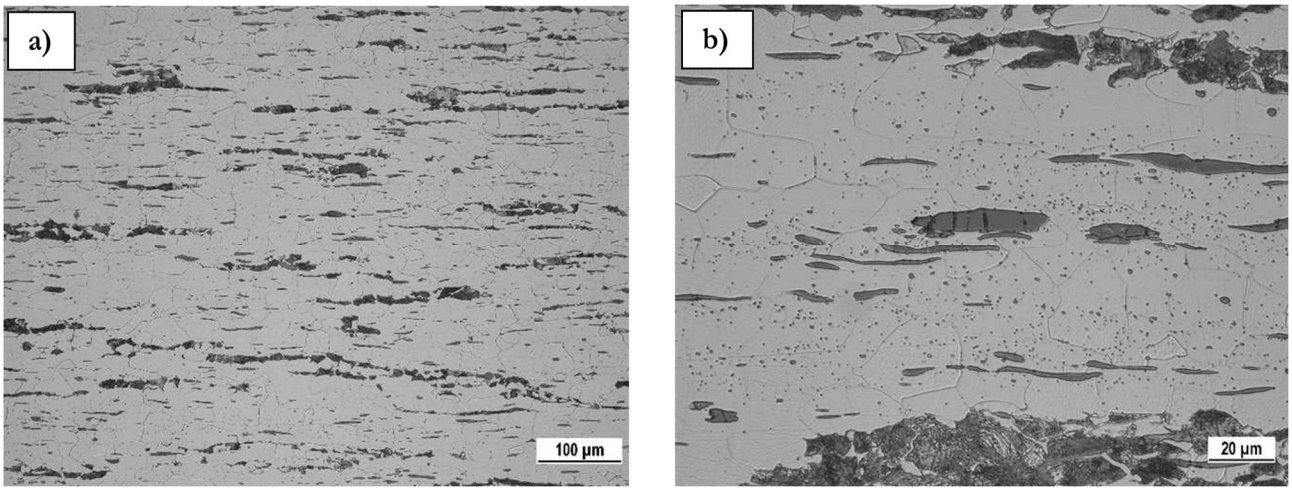

Fig. 1 *a) Microstructure of 11SMn30 steel, b) detail of elongated sulphide formations*

The comparison showed that the experimental material corresponds to the standard in terms of its chemical composition. The next step to define the initial state of the experimental material was to examine the microstructure. To be able to determine the different structures and substructures in the material, two types of microscopes were used.

Before microstructural observation, the material

was metallographically prepared in five subsequent steps (sampling, preparation, grinding, polishing, etching). Prepared specimens were observed using a NEOPHOT 32 light microscope. Observations of substructures, details and fractures were performed using a TESCAN LMU II scanning electron microscope equipped with Bruker EDX analyser which allows the concentration of chemical elements to be determined in a selected area [9, 10].

After polishing, only elongated long sulphidic formations can be observed, in the structure of the steel which follows the rolling direction. For making grain boundaries visible the 3% Nital etchant was used. After etching, the ferrite-pearlite microstructure with a high content of elongated sulphides typical for free-cutting steel was observed. The ferrite grains form a meshwork, are of different sizes and are partially deformed (Fig.1).

Pearlite appears dark in light microscopy because it is a eutectoid mixture of ferrite and cementite (Fig. 1b). A substantial part of the sulphides present has been rolled into small formations during the hot rolling production process which forms regular clusters in the structure. Microcracks also occur within some of the larger sulphides (Fig. 1b). A surface EDX microanalysis (mapping) was used to analyse non-metallic inclusion occurring in the structure. It was confirmed that the sulphides present are manganese - MnS based. In addition, remnants of segregated tertiary cementite were also present at some locations along the grain boundaries.

The observed microstructure of experimental steel gives the first indications of the mechanisms by which the steel may be attacked when in contact with a hydrogen environment. At the sites of sulphides, oxides or other non-metallic inclusions, and grain boundaries, "hydrogen traps" can be formed at sites with higher internal stress concentrations, as reported in [1, 11]. The sites with internal stresses are most often the grain boundaries and the interface between the inclusions and the matrix of the metal. At grain boundaries, recombining of atomic hydrogen into molecular hydrogen can occur if it is energetically advantageous at that location and the hydrogen atoms have a strong affinity for holding onto valence electrons [1, 11].

3 Experimental methods

The chosen hydrogenation process reflects possible causes of hydrogen embrittlement from practice. For example, during material production, especially heat treatment, during various surface treatments of final products, and also in the operation of manufactured components hydrogenation can take place. It is necessary to simulate the conditions so that they are as close as possible to a real-life scenario.

3.1 Immersion hydrogenation method

The immersion hydrogenation method was chosen based on theoretical knowledge of hydrogen embrittlement, which states that during immersion hydrogenation, the amount of hydrogen adsorbed to the material is sufficient to induce embrittlement. At the same time, this procedure is more practical than cathodic hydrogenation. Tagaki S. and Toji Y. [12] state that the use of ammonium thiocyanate is the most suitable choice for immersion hydrogenation. Its advantage is, among other things, that the loss of materials in g/cm² is practically zero regardless of the immersion time. From an experimental point of view, immersion hydrogenation is simple and fast (Fig. 2).

Fig. 2 *Set up for immersion hydrogenation of specimens in NH_4SCN water solution*

For immersion hydrogenation, a solution of 20% NH_4SCN in distilled water was used, which, according to the authors Tagaki S. and Toji Y., hydrogenated the material intensively within 50 hours. The solution was prepared by mixing 500 g of ammonium thiocyanate with 2 litres of distilled water. The beakers used had to be sized to accommodate the placement of the samples in the solution. Immersion hydrogenation of the specimens was carried out in the fume cupboard for 50 hours [12].

3.2 Cathodic hydrogenation method

The process is conditioned by the moment when the source creates a potential difference and initiates positive hydrogen ions, which move from the electrolyte to the experimental material - the cathode. The flow of charged particles creates a layer of

hydrogen on the surface of the test specimen. An experimental setup has been constructed for this method (Fig. 3).

The cathodic hydrogenation method is based on the principle of electrolysis. The process involves a cathode represented by the experimental material and a platinum anode. To simulate the hydrogenation of the electroplated material a zinc anode was also used. The cathodes did not have standardized dimensions. The DC supplied to the electrolyte initiates decomposition accompanied by the formation of hydrogen ions - specifically hydrogen protons. The 0.5 M H_2SO_4 solution with the addition of 0.28 g of thiourea NH_2CSNH_2 per 0.5 litre of solution was used as an electrolyte. Insulating shrinkage strips were introduced on the specimens to reduce the hydrogenated area to the notched area, see Fig. 3. Used parameters of cathodic hydrogenation are listed in Tab. 3.

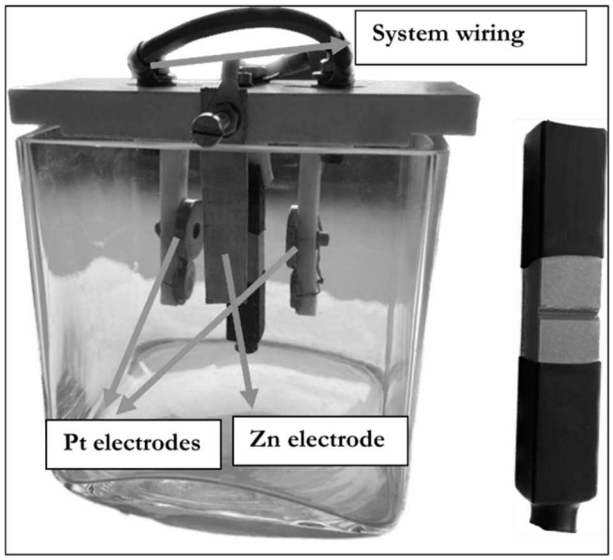

Fig. 3 *Experimental apparatus for cathodic hydrogenation (left side) and detail of the test specimen (right side)*

Tab. 3 *Parameters of cathodic hydrogenation*

Current density (mA/ cm²)	Set parameters		Temperature (°C)	Time (hours)
	Current (A)	Voltage (V)		
100	1.7	3.0	32	24

4 Result and discussion

4.1 Impact bending test before hydrogenation

The dimensions, geometry and surface quality of the experimental specimens for the Charpy test were used according to EN 10045-1 standard. The impact test was performed using a Charpy pendulum with a maximum impact energy of 300 J. Both parts of the specimen were immediately transferred to the desiccator after the impact test. The frozen specimens (-70°C) were immersed in alcohol and then dried with a stream of hot air to prevent flash corrosion of the fracture surfaces. The specimens in the initial state before hydrogenation were tested at 20°C and -70°C to determine their toughness before hydrogenation. The absorbed impact energy recorded at both temperatures was very low, namely 11 Joules at 20°C and 2 Joules at -70°C. In general, free-cutting steels are characterised by low impact toughness caused by a high content of sulfidic inclusions and therefore these steels have not guaranteed impact toughness. After the Charpy impact test, the fracture character was evaluated using a scanning electron microscope. Fig. 4 shows a fracture of a specimen broken at 20°C. The areas marked by numbers 1 and 2 show the locations describing the type of failure.

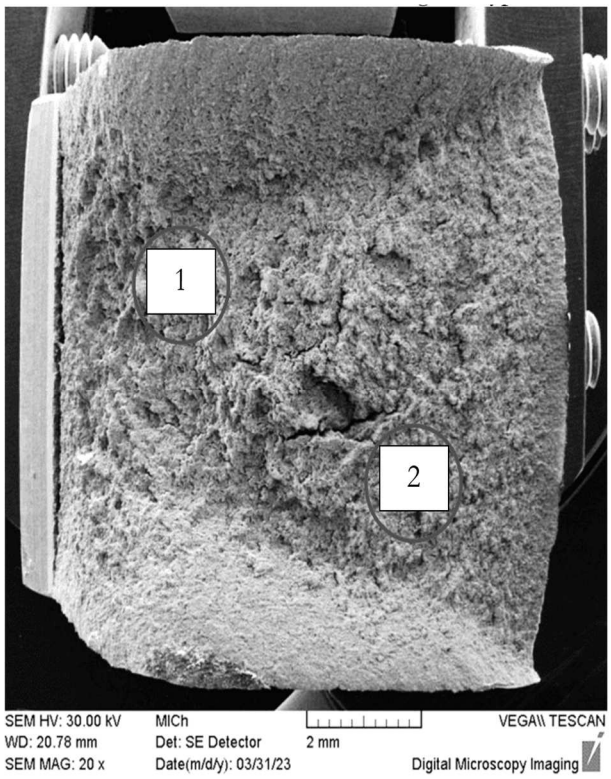

Fig. 4 *Impact fracture of 11SMn30 steel at 20°C before hydrogenation*

ISSN 1213–2489
e-ISSN 2787–9402

The detailed view (Fig. 5a) of area 1 from Fig. 4 shows locations describing ductile fracture with dimple morphology. Detail of area 2 (Fig. 5b) shows transcrystalline ductile fracture with dimple morphology where either broken sulphide (MnS) or cementite particles are present at the bottom of the dimples. The abundance of sulphidic particles is related to the high sulphur content and their shape and distribution are determined by the rolling of the semi-finished product.

The pits are irregular with several sulphides. The type of inclusions was detected using a Bruker EDX spectrometer in mapping mod (Fig 6).

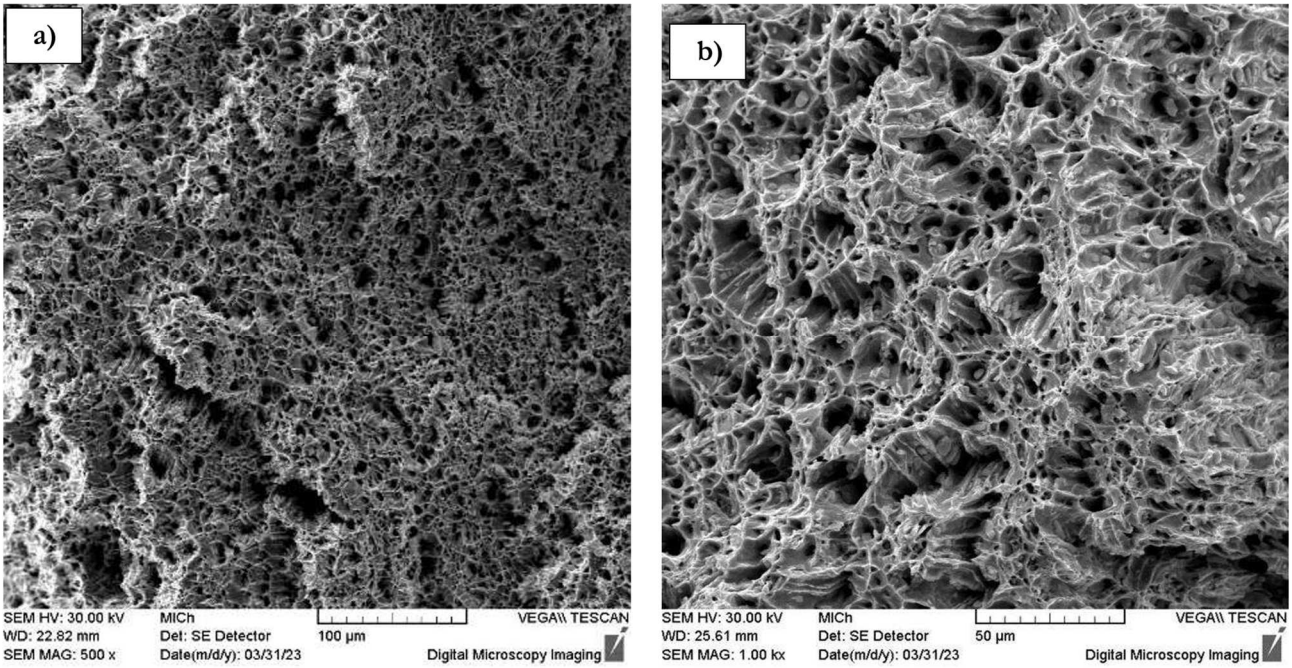

Fig. 5 *a) Impact fracture of 11SMn30 steel at 20°C before hydrogenation, b) detail of transcrystalline ductile fracture the presence of sulphides*

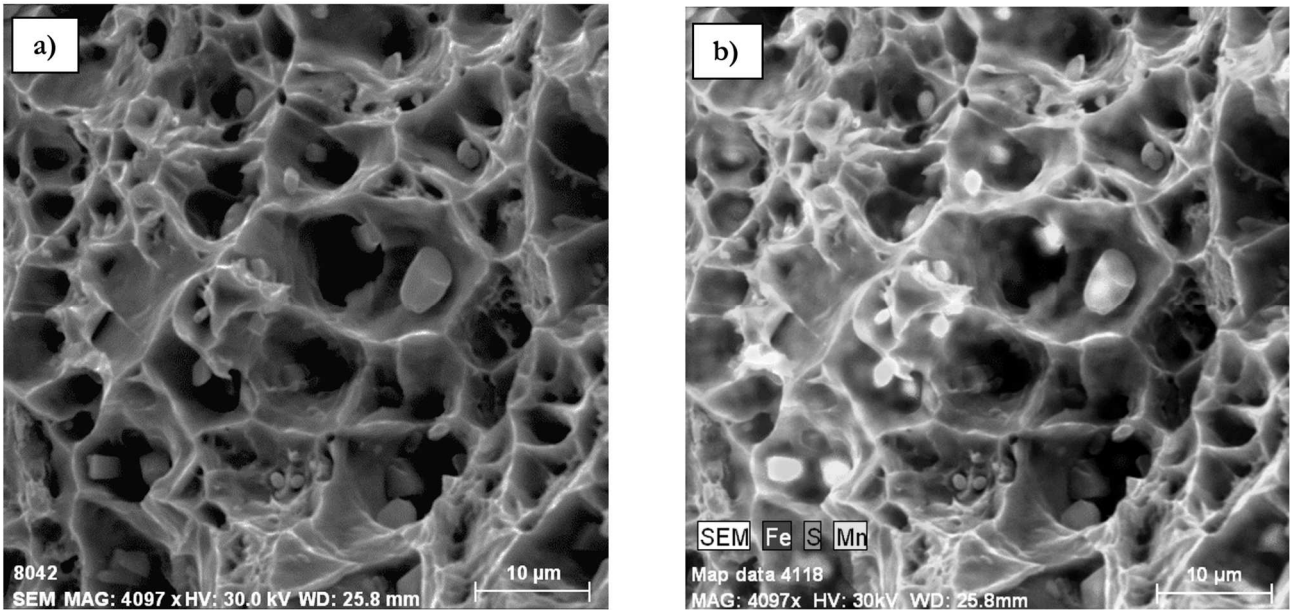

Fig. 6 *a) Detail of analysed particles at the bottom of the dimples, b) distribution of assessed elements in the analysed area*

3.1.2 Analysis after plasma nitriding

In specimens tested at -70°C, the failure mechanism changed from ductile to cleavage. The rigorous decrease in plastic deformation and embrittlement of the material due to the effect of blocked dislocation cross slip at low temperatures is evident. There were observable cleavage facets with river morphology. Secondary cracks indicate

weaknesses in the material structure. There are several areas of different fracture character on the fracture surface. In area 1 (Fig. 7a) above the crack initiation, the fracture has a mixed character (ductile and quasi-cleavage fracture). A quasi-cleavage fracture accompanied by secondary cracks with different orientations occurs on the fracture surface in area 2 (Fig. 7b).

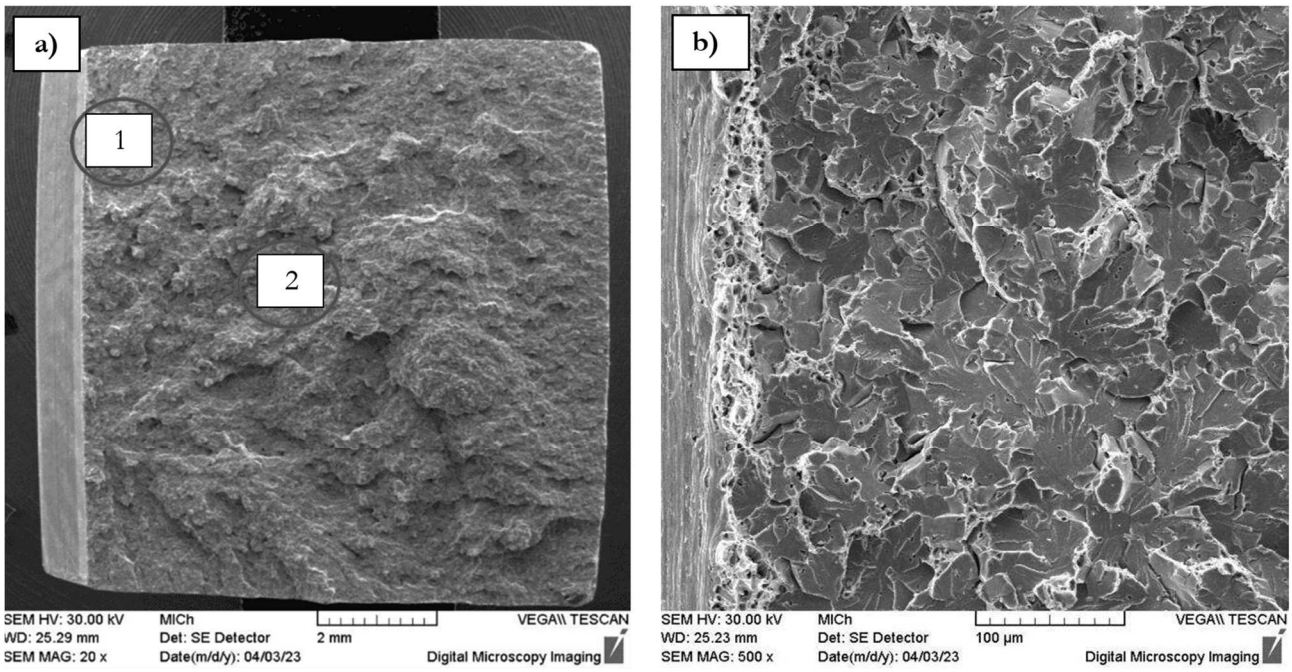

Fig. 7 *a) Impact fracture of 11SMn30 steel at -70°C before hydrogenation, b) (area 1) detail of quasi-cleavage transcrystalline fracture*

In most of the fracture locations, mixed fracture with a combined failure mechanism was present. A detail of the mixture of transcrystalline quasi-cleavage fracture, intercrystalline cleavage fracture and transcrystalline ductile fracture can be seen in Fig. 8a. The detailed view (Fig. 8b) shows the cleavage facets having a river morphology and the intercrystalline microcracks along the grain boundaries.

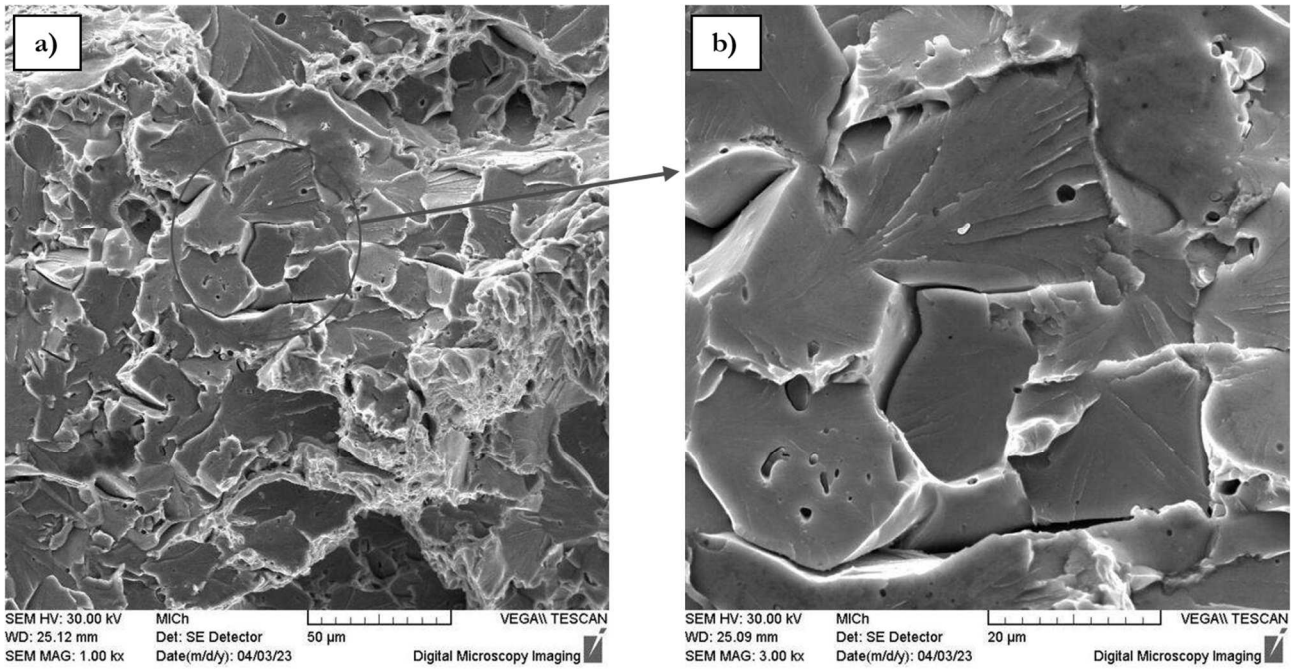

Fig. 8 *a) impact fracture of 11SMn30 steel at -70°C before hydrogenation - mixed fracture consisting of transcrystalline quasi-cleavage fracture, intercrystalline cleavage fracture and transcrystalline ductile fracture (area 2), b) detail of intercrystalline microcracks and river morphology of cleavage facets*

4.2 Impact bending test after hydrogenation

4.2.1 Analysis of fracture surfaces after Immersion Hydrogenation

The absorbed impact energy of the 11SMn30 steel recorded at 20°C drops after hydrogenation to 8 Joules.

The fracture surface of this steel tested after immersion hydrogenation has a predominantly ductile character with dimple morphology (Fig. 9a, b), but in some areas, a mixture of ductile and quasi-cleavage fracture can be observed also (Fig. 10 a, b). The local occurrence of quasi-cleavage fracture, differently oriented secondary cracks and intercrystalline microcracks indicate that the material becomes brittle due to the presence of hydrogen atoms. In addition to the fact that the failure mechanism of the material has been significantly altered, there are also many secondary cracks in the ductile region (Fig. 9a). Compared to the non-hydrogenated steel, there were many more secondary cracks with a high probability of their orientation along grain boundaries. This fact lends credence to the assumption that the material was embrittlement due to the influence of immersion hydrogenation.

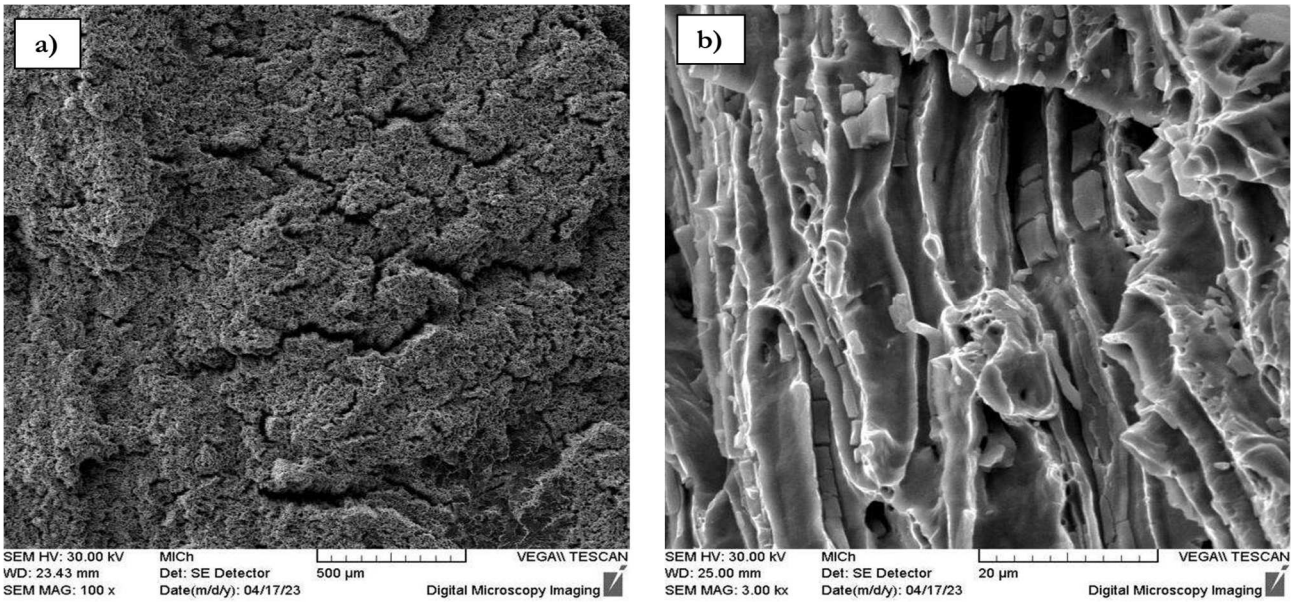

Fig. 9 *a) Impact fracture of 11SMn30 steel at 20°C after immersion hydrogenation - transcrystalline ductile fracture with dimple morphology and secondary cracks, b) detail of elongated dimples with long sulphidic particles at the bottom*

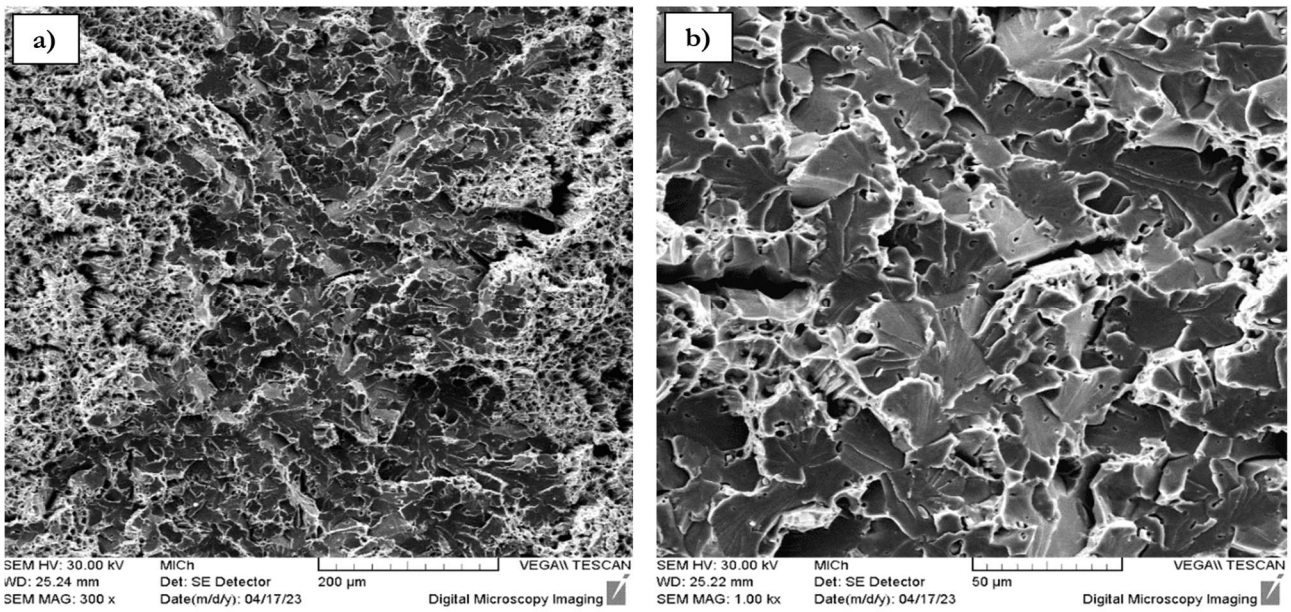

Fig. 10 *a) Impact fracture of 11SMn30 steel at 20°C after hydrogenation - mixture of transcrystalline ductile fracture and transcrystalline quasi-cleavage fracture, b) detail of transcrystalline quasy-cleavage fracture and the occurrence of intercrystalline microcracks*

4.2.2 Analysis of fracture surfaces after cathodic hydrogenation

Due to the attack of cathodic hydrogenation absorbed impact energy of the 11SMn30 steel tested at 20°C drops to 4 Joules. After hydrogenation in the electrolytic solution, there was observed also a significant change in the fracture mechanism. Along the perimeter of the specimen, the material fails by ductile fracture (Fig. 11a, b). At these locations, ductile fracture with dimple morphology occurs. Investigation of the central part of the fracture (area 1) revealed that the failure mechanism changed from ductile to cleavage fracture (Fig. 12a, b). Compared to immersion hydrogenation, the area of brittle fracture is much bigger in the case of cathodic hydrogenation [13]. The cleavage fracture mechanism is predominant in this case, similar to the fracture of non-hydrogenated steel broken at -70°C. This behaviour is a significant indication of hydrogen embrittlement.

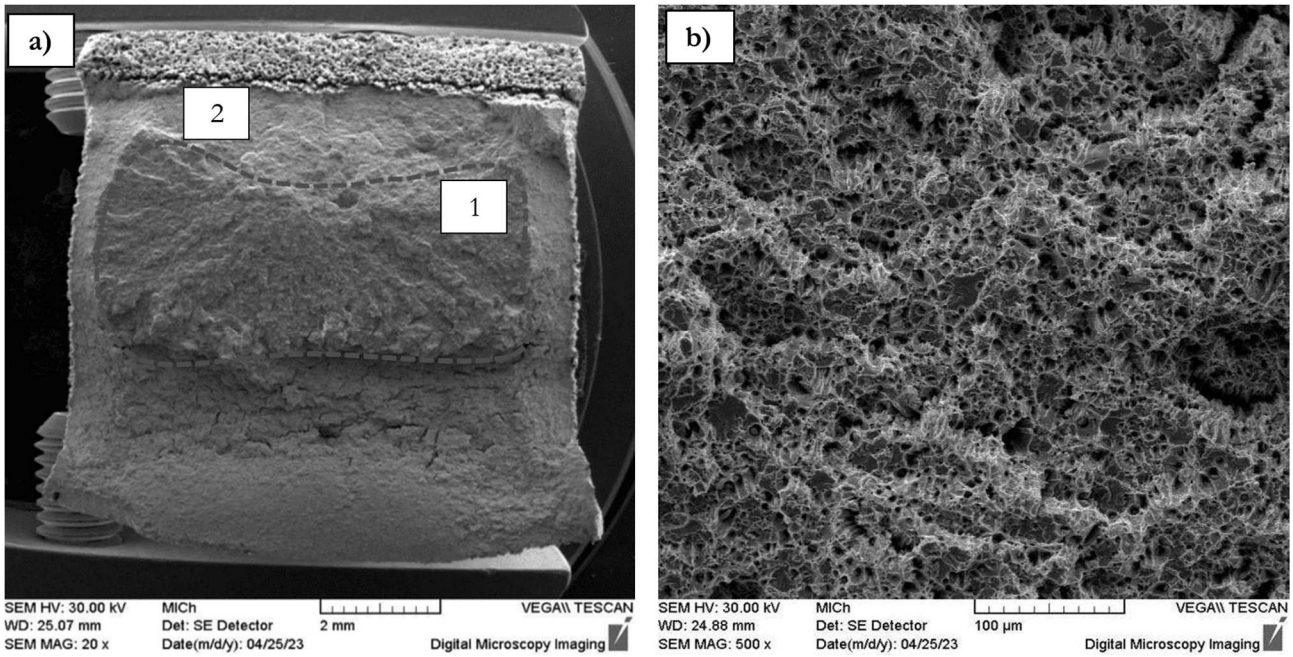

Fig. 11 *a) Impact fracture of 11SMn30 steel at 20°C after cathodic hydrogenation - general view of the fracture surface, b) area 2- ductile fracture aroud the perimeter of the specimen*

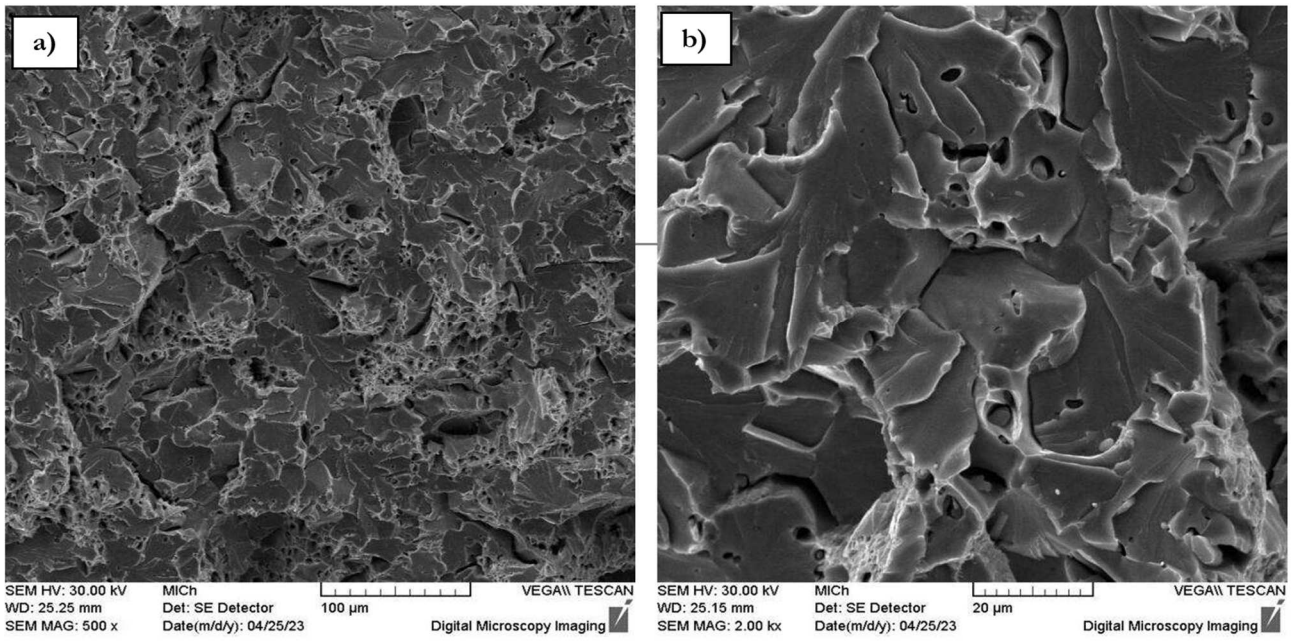

Fig. 12 *a) Impact fracture of 11SMn30 steel at 20°C after cathodic hydrogenation - mixture of transcrystalline quasi-cleavage fracture with local occurrence of transcrystalline ductile fracture and secondary cracks (area 1), b) detail of predomination of quasi cleavage fracture*

5 Conclusion

The material used in this work was chosen based on its use in complex shape components with threads. Those are mainly used in hydraulic systems – stationary or mobile, that may be exposed to atomic but mainly molecular hydrogen.

The results reported in this paper indicate that manganese sulphide inclusions are not the main cause of hydrogen embrittlement in free-cutting steels. The effect of manganese sulphide inclusions was attributed to hydrogen trapping, which generated a high stress causing their decohesion from the matrix. The main cause for hydrogen embrittlement in free-cutting steels seems to be the blocking of dislocation cross slip due to the hydrogen presence in the structure. The objectives of the study were met, but to fully understand the issues, the experiments require a significantly longer period and more complex preparation. The 11SMn30 free-cutting steel has to some extent shrunk due to the diffusion of atomic hydrogen. It is difficult to determine which method is more suitable for experimental purposes, but from a practical and economic point of view, immersion hydrogenation is preferable. However, it appears from the results that a greater probability of hydrogenation can be achieved using cathodic hydrogenation.

Obtained results show that proper care must be taken in the selection of the material for the specific conditions of its use in practice.

Acknowledgement

The research was funded by the Slovak Research and Development Agency under contract No. APVV-20-0427 and the Slovak Ministry of Education, Science, Research, and Sport's Scientific Grant Agency under contract VEGA No. 1/0741/21.

This research was supported by HYDAC Electronics s.r.o., which supplied the specimens.
Furthermore, ***the paper served as an information resource for the company.***

References

[1] SOJKA, J., (2007). Resistance of steels to hydrogen embrittlement (CZ). Ostrava: VŠB-TUO, 2007. ISBN 978-80-248-1648-7.

[2] KREIBICH, V., (1992) Corrosion and surface treatment technology (CZ). Praha: ČVUT. ISBN 80-01-00750-2.

[3] CAMBELL, F., (2012) Fatigue and fracture: understanding the basics. Materials Park, Ohio: ASM International. ISBN 978-1-61503-976-0.

[4] JANOVEC J., (2004) Physical metallurgy (CZ). Praha: Vydavatelství ČVUT. ISBN 80-01-02935-2.

[5] Staněk B, a i. Steel Manufacturing Program, Volume II Properties and Applications Volume 3 (CZ). 1980 Praha: TOMOS Praha

[6] STEELS (SK) [Online] (2020). from: http://kmi2.uniza.sk/wp-content/uploads/2020/01/3_Ocele-1.pdf

[7] Free-cutting steel [Online] (2020). from: https://steeltec-group.com/en/products-solutions/free-cutting-steels#panel1

[8] BELAN, J., VAŠKO, A., KUCHARIKOVÁ, L., TILLOVÁ, E., CHALUPOVÁ, M. (2019). The SEM Metallography Analysis of Vacuum Cast ZhS6K Superalloy Turbine Blade after Various Working Hours. In: *Manufacturing Technology*. Vol. 19. No. 5. pp. 727-733. ISSN: 1213-2489

[9] BELAN, J., VAŠKO, A., KUCHARIKOVÁ, L., TILLOVÁ, E., MATVIJA, M. (2018). The High-Temperature Loading Influence on Orthorhombic Ni_3Nb DO_a δ-Phase Formation and its Effect on Fatigue Lifetime in Alloy 718. In: *Manufacturing Technology*. Vol. 18. No. 6. pp. 875-882. ISNN: 1213-2489

[10] VAŠKO, A. BELAN, J., TILLOVÁ, E. (2020). Use of Colour Etching in the Structural Analysis of Graphitic Cast Irons. In: *Manufacturing Technology*. Vol. 20. No. 6. pp. 845-848. ISSN: 1213-2489

[11] HYSPECKÁ L., 1978 Hydrogen embrittlement of higher parameter structural steels (CZ). Praha: Academia. Studie ČSAV.

[12] TAGAKI, S., 2012. Application of NH4SCN Aqueous Solution [Online] ISIJ International, [cit. 04.11.2022] dostupné z: https://www.semanticscholar.org/paper/Application-of-NH4SCN-Aqueous-Solution-to-Hydrogen-Takagi-Toji/bcc9c5f2e0072343f374e9487a2a3eda2707c148

[13] ŠIKYŇA, L., (2023) Effect of hydrogen saturation on the properties of selected steels, *Master thesis* (SK).